Pharmaceutical Research, Vol. 24, No. 1, January 2007 (© 2006)
DOI: 10.1007/s11095-006-9118-y

Research Paper

Raman Mapping of Low-Content API Pharmaceutical Formulations. I. Mapping of Alprazolam in Alprazolam/Xanax Tablets

Slobodan Šašić[1,2]

Received May 11, 2006; accepted July 10, 2006; published online October 18, 2006

Purpose. Raman chemical imaging of API was carried out to provide information on whether there is any structural difference between the commercial Xanax™ and Alprazolam™ tablets (the API content less than 1% w/w in both cases) in the batches with low and good recovery.
Materials and Methods. Raman mapping spectra were collected from the flattened surfaces of six tablets. The mapping spectra were analyzed by principal component analysis because the Raman signal of the API (Alprazolam) was not reliably detected from the raw spectra. The complexity of the obtained grey-scale score images was such that no information about the domain sizes of the API could be obtained and thus binarization was applied to simplify these images.
Results. It was found that reliable detection of the Raman signal of the API was only achieved after principal component analysis was employed with the mapping being facilitated by a surprising similarity between a high principal component loading and the spectrum of the API. The binarization was successful only if the outlying pixels in the score images are eliminated.
Summary. The final chemical images represent quantitative characterization of the domains of the API in the tablets in contrast to chemical images of tablets that have been reported so far in the literature which have usually been descriptive only. The abundance of Alprazolam in all six tablets of Xanax and Alprazolam, respectively, was very similar. The domain sizes were found to be below 75 μm in diameter for all the tablets analyzed.

KEY WORDS: Alprazolam; chemical imaging; chemical mapping; chemometrics; principal component analysis; Raman; Xanax.

INTRODUCTION

Raman spectroscopy has been actively used for analysis of solid dosage pharmaceutical formulations (1–8). Its strong points include negligible sample preparation and distinctness of Raman spectra; these are much less overlapped than near-infrared (NIR) spectra which are more frequently used for analyzing pharmaceutical samples. A particularly valuable aspect of Raman spectroscopy is that active pharmaceutical ingredients (APIs) tend to have strong Raman response which makes their detection possible even when present at low concentration. However, this feature has not been actively exploited for determining spatial distribution of APIs in the tablets and the major aim of this study is to demonstrate the capability of Raman spectroscopy for visualizing minor amount of API in solid dosage pharmaceuticals via Raman chemical mapping.

A Raman mapping experiment refers to the collection of a matrix of Raman spectra via automated shifts of the microscope stage of the Raman mapping instrument equipped with point or line laser excitation (9–11). Chemical images can then be produced from the acquired spectra (with tagged spatial coordinates) in various ways. The simplest option is to follow the intensity variation at the wave numbers that are uniquely assignable to the components of the material being imaged. This so-called univariate approach is used whenever possible because it is the simplest and most understandable way to produce chemical images, one for each component. However, the condition that all the components of the imaged sample have uniquely assignable wave numbers with satisfactory signal-to-noise (s/n) ratio is not always fulfilled. Thus, advanced data analysis tools such as principal component analysis (PCA; 12–15) are used for extracting the Raman signal that is seemingly buried in noise in the original spectra. Multivariate curve resolution has also been shown to be very effective for unravelling complex spectral data from mapping (or imaging) Raman data (16–19).

The combination of Raman chemical mapping and chemometrics has not been used, as far as the author is aware, for determining the precise spatial distribution of minor amounts of APIs in commercial tablets (minor amounts of API are most frequently used in formulations). Chemical images of solid dosage pharmaceuticals have been reported (10) but the imaged components were present in relatively high concentration and close inspection of the

[1] Analytical R&D, Pfizer Global Research and Development, Ramsgate Road, Sandwich CT13 9NJ, UK.
[2] To whom correspondence should be addressed. (e-mail: slsasic@yahoo.com)

obtained images was not carried out. In other words, the chemical images of the tablets were just displayed but not quantified in terms of characterization of their features (such as defining domain sizes, for example).

The aim of this study is to precisely determine the spatial distribution of Alprazolam (the name of the API) in commercial 0.5 mg Xanax™ and 1.0 mg Alprazolam™ tablets (the API content less than 1% w/w in both cases). Two batches of both Xanax and Alprazolam tablets were analyzed. In the case of each type of tablet one of the batches was known to have low recovery. Chemical imaging of Alprazolam was carried out to provide information on whether there is any structural difference (regarding the API) between the tablets in the batches with the low and good recovery. NIR imaging was also attempted but it failed because the signal of Alprazolam was too weak in the NIR region.

It is demonstrated here that the above task cannot be solved without applying multivariate data analysis tools because the Raman signal of Alprazolam is too weak to be used for univariate imaging. Also, interesting observations are reported in relation to the handling of the obtained chemical images. The chemical images displayed here are visually very complex and have to be simplified, usually via binarization. The problems encountered during binarization of chemical images are easily solved after inspecting the grey-scale Raman chemical images on outlying pixels. However, the elimination of bad pixels is not trivially carried out by commercial imaging software and thus in-house written routines are used.

EXPERIMENTAL

The Xanax and Alprazolam tablets contained 0.4 and 0.8% (w/w) of Alprazolam, respectively. The most abundant excipient was lactose (78%) followed by starch. Other excipients were present but at much lower concentration. The bulk spectrum of both types of tablets was very similar to the spectrum of lactose.

Raman mapping spectra were collected on a Renishaw Ramascope System 1000 using Wire V.1.3 software. The spectra were obtained by exciting the sample with a laser line at 782 nm. The samples were viewed and Raman data collected through a ×20 objective. The data collection was set to cover the ca. 550–1,120 cm^{-1} range. The spatial resolution in the X dimension was 25 μm, set by the experiment stepsize. In the Y dimension the resolution was 27 μm because the laser line was fully binned so that this experiment was effectively equivalent to the experiment with a point laser source. A typical chemical image comprised 78×81 pixels. The spectra were acquired for 10 s per stage position resulting in total acquisition time of about 24 h. The acquisition time could have been shortened down to 5 s with perfectly satisfactory spectra still being obtained. However, the total acquisition time does not change linearly with the acquisition time because the stage settling time takes several seconds so that halving the actual acquisition does not lead to half the total acquisition time. In addition, there was no software handle to turn the laser off at the end of acquisition (e.g., if the acquisition terminates during the night). Thus, it was impractical to reduce the acquisition time of 10 s.

Commercial tablets were used for all experiments. The only treatment applied to the tablets was trimming to ensure that a flat surface was available for analysis.

The spectra were imported into the chemical imaging software, ChemAnalyze (ChemImage, Pittsburgh, PA) where PCA was carried out. Before PCA, the spectra were baseline corrected with a first order polynomial passing through three selected segments. The images created in ChemAnalyze were then exported into Matlab (Mathworks, Natick, MA) and further refined by using a series of separate Matlab commands. All the binarized images in this report were created in Matlab.

RESULTS AND DISCUSSION

Xanax Tablets

Figure 1 displays the Raman spectra of the most important constituents of the Alprazolam/Xanax tablets. The strongest band of Alprazolam is centered at about 1,000 cm^{-1} but it cannot be used for mapping purposes (as a univariate wave number) because of the overlap with the bands of docusate sodium and lactose, components which are present at much higher concentration. The best wave number region for determining Alprazolam bands is thus considered to be between 620 and 720 cm^{-1} despite the presence of the lactose band at 633 cm^{-1}. The spectra were therefore truncated so that only the 580–720 cm^{-1} region was analyzed.

The Raman chemical image created at the position of the strongest Alprazolam peak in the region, at 687 cm^{-1}, for one of the Xanax tablets is shown in Fig. 2A. It is very difficult to extract useful information from this image because the white pixels that are supposedly correlated with Alprazolam (the stronger the Raman signal of Alprazolam, the 'whiter' a pixel) are spread all over the area mapped. In addition, as argued in our previous publication (11), it should not be supposed that the white pixels necessarily indicate a strong Raman signal due to Alprazolam. Since this API is present at a low concentration in the formulation investigated, its signal might not be detected which would mean that actually only noise is shown in Fig. 2A, not the spatial distribution of Alprazolam. This assumption can be verified by inspecting the spectra at randomly chosen white pixels. Mapping instruments normally collect the spectra with the spatial coordinates precisely defined and the chemical images are produced later on using data via univariate or multivariate approaches. Thus, each pixel is associated with a Raman spectrum allowing inspection of the raw spectra from which the image in Fig. 2A is produced. Figure 2B reveals that the Raman spectra that give rise to the white pixels are not associated with the Alprazolam in a straightforward manner because the spectral features of Alprazolam (Fig. 1) are not recognized in all the spectra that give rise to the white pixels. It transpires that simple univariate imaging does not provide reliable maps of Alprazolam. Moreover, if the Raman mapping spectra behind the chemical image are not verified in some way this approach can be misleading by effectively failing to distinguish between signal and noise.

This problem may be overcome by applying more advanced tools for data analysis such as PCA. The general

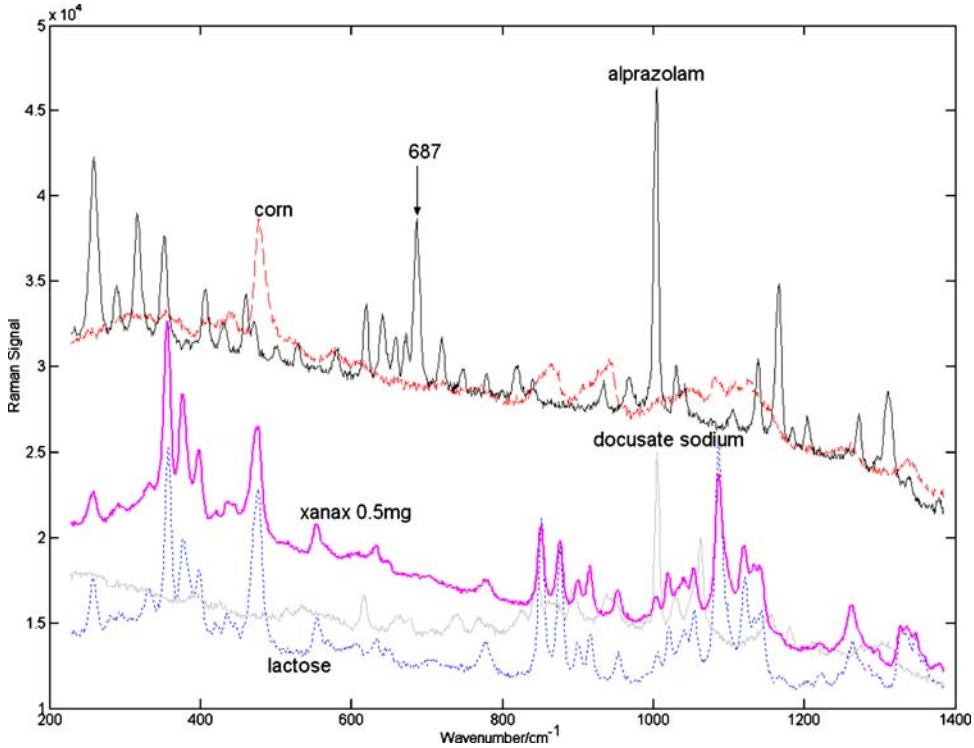

Fig. 1. The spectra of Alprazolam (*API*) and major excipients of Xanax and Alprazolam tablets. Also shown is a typical spectrum of a Xanax tablet obtained through the microscope. Note its similarity with the lactose spectrum.

aim of PCA is to eliminate noise and search for the spectral signatures of Alprazolam in the PC loadings. Although it should not be expected that these signatures are easily identifiable, at least one can evaluate whether there is any recognizable signal due to the Alprazolam bands.

The PCA results are very surprising. The fourth loading (Fig. 3) almost exactly matches the spectrum of Alprazolam which means that the corresponding re-folded score represents the spatial distribution of Alprazolam. This similarity is quite exceptional because the loadings are linear combinations of the pure component spectra and thus normally do not correspond directly to the spectra. Furthermore, the first three loadings feature either the lactose bands or are difficult to define, and then, unexpectedly, the fourth loading closely matches the Alprazolam spectrum. If the rules for retaining/eliminating the principal components were followed, the fourth loadings would be considered as noise and eliminated from further analysis. Typical eigenvalues for the mean-

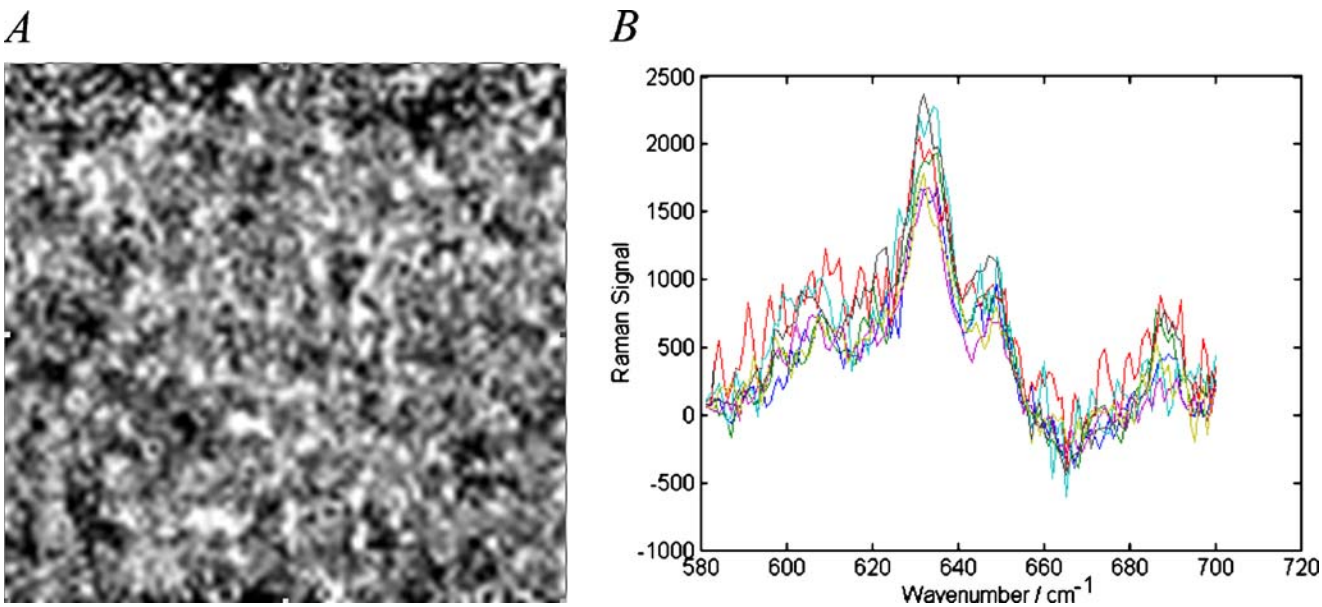

Fig. 2. Univariate image (2×2 mm^2) of Alprazolam at 687 cm^{-1} (A). Raman spectra from randomly selected white pixels (B).

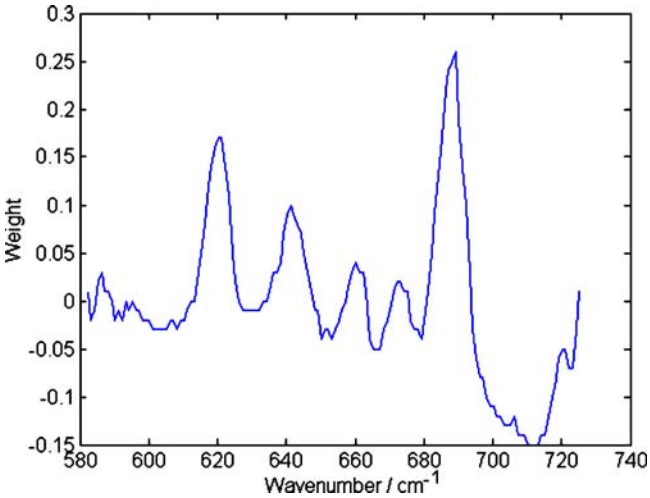

Fig. 3. The fourth PC loading obtained by PCA of the Raman mapping spectra from a Xanax tablet. Note the similarity between the shown PC loading and spectrum of Alprazolam in Fig. 1.

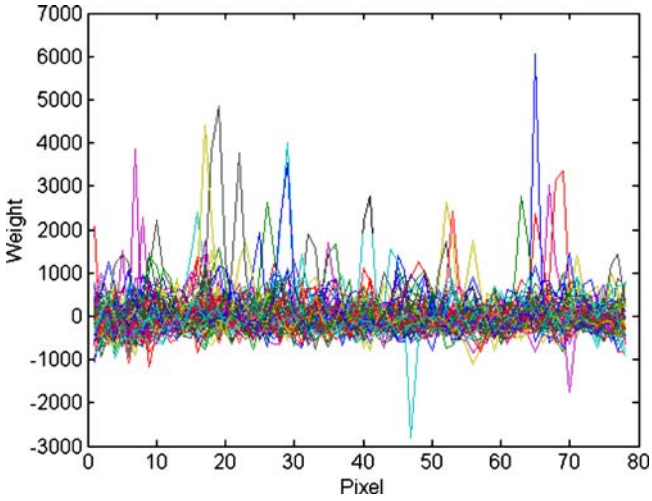

Fig. 5. One-dimensional representation of the image in Fig. 4.

centered data are 58.9, 6.1, 3.8, 1.3, 0.9, 0.8, 0.7, 0.6, 0.5, ... and eigenvalues-based criteria for s/n threshold suggest that only the first PC is to be retained. The fortunate correlation between the low-variance PC loadings and the Alprazolam spectrum allows us to produce the images of Alprazolam in all six Xanax tablets investigated. For all these tablets the PCA results are similar.

The PC4 score image of Alprazolam shown in Fig. 4 is very complex and the only straightforward conclusion that can be reached is that Alprazolam appears to be finely spread, i.e., big and isolated domains of Alprazolam are not seen. It is necessary to simplify Fig. 4 to learn more from it, the more so as it should be kept in mind that the fourth PC loading that features Alprazolam covers only a very small amount of variance in the data set and is thus susceptible to the effects of noise.

The grey-scale image in Fig. 4 was produced by the imaging software. The difference in the whiteness of the pixels is not apparent and thus one cannot select pixels that reflect a high content of Alprazolam. Attempts to binarize Fig. 4 do not yield a valuable result as the 'on' pixels in the binarized image occupy 40% of the total number of pixels in the image, indicating an unreasonably high proportion of Alprazolam in the tablet (100 times greater than the nominal weight percentage and in sharp contrast to the inherent weakness of the signal). This effect is caused by ineffective setting of the binarization threshold. The binarization threshold can be manipulated through software in order to reduce the number of Alprazolam pixels but such an operation is highly subjective if the raw image data are not analyzed beforehand. The image in Fig. 4 is thus plotted in one-dimensional form, 78 lines with 81 data points and these are shown in Fig. 5.

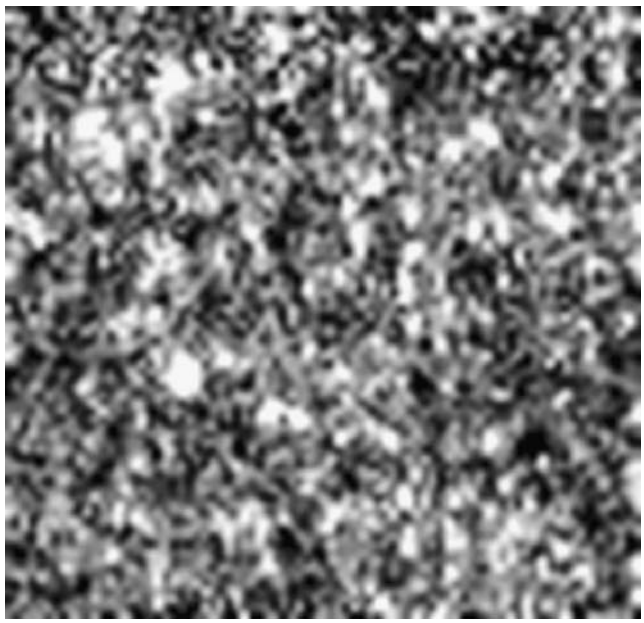

Fig. 4. The PC4 score image that, correspondingly, features Alprazolam. The size of the image is 2×2 mm^2 which is about 50% of the imageable area on the tablet.

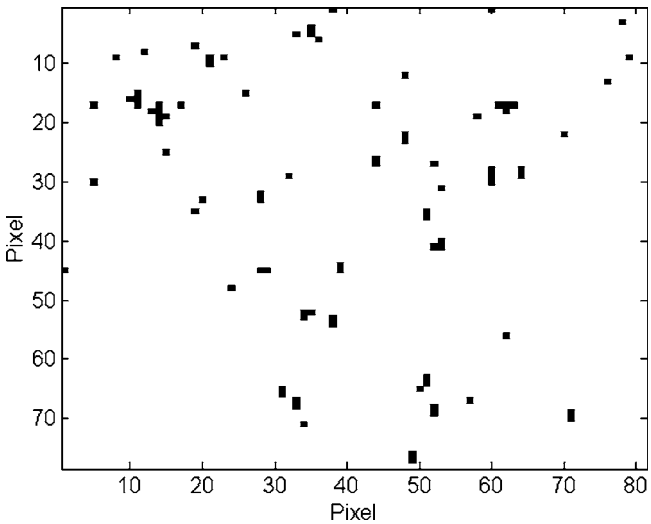

Fig. 6. Binarized image of Fig. 4 after the two outliers in Fig. 5 have been removed. The *black pixels* in this and all other binarized images throughout refer to the API.

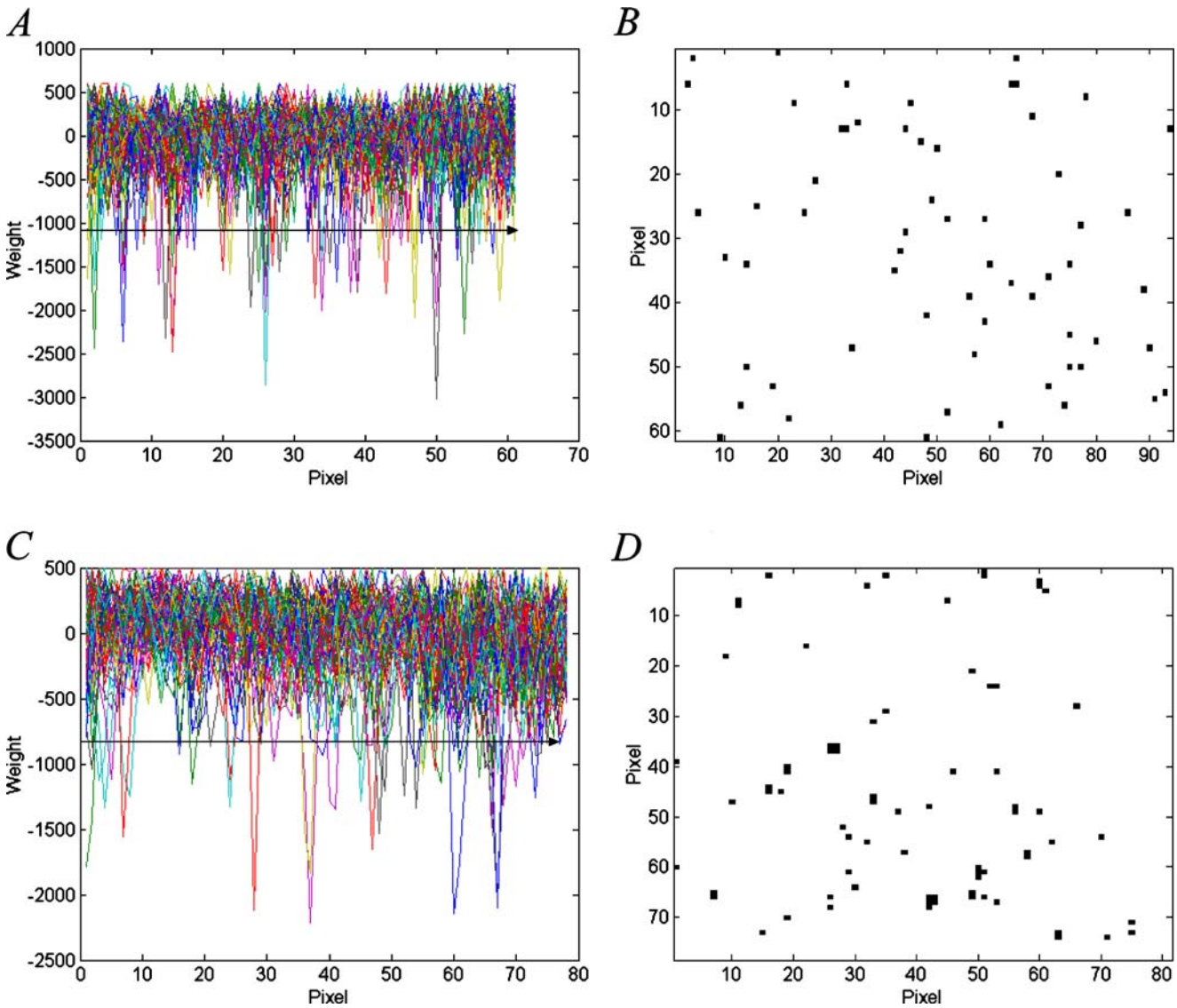

Fig. 7. The illustrations of threshold and binarized images for the second (A and B) and third (C and D) Xanax tablets.

Figure 5 reveals that there are two outlying negative data points that obstruct the appropriate setting of the binarization threshold. These two negative peaks set the threshold at far too low a level so that many noisy data points are considered as 'on' pixels and thus Fig. 4 is too complex and gives the wrong impression. After these negative peaks are eliminated and the binarization threshold is (arbitrarily) set at 1,000, Fig. 6 is produced. The binarization threshold allows only the data in the upper 65% of the intensity scale to be shown. The image in Fig. 6 is now certainly based on the relatively strong Raman signal of Alprazolam. There are about 1% of the pixels in this image that are assigned to Alprazolam which is about twice the actual percentage of Alprazolam in the tablet formulation. However, for various reasons it should not be assumed that the percentage of pixels assigned to a component in a chemical image exactly corresponds to the weight percentage of that component so that the obtained number of pixels is acceptable. The most important information to be extracted from Fig. 6 is the domain size. It transpires that Alprazolam is distributed

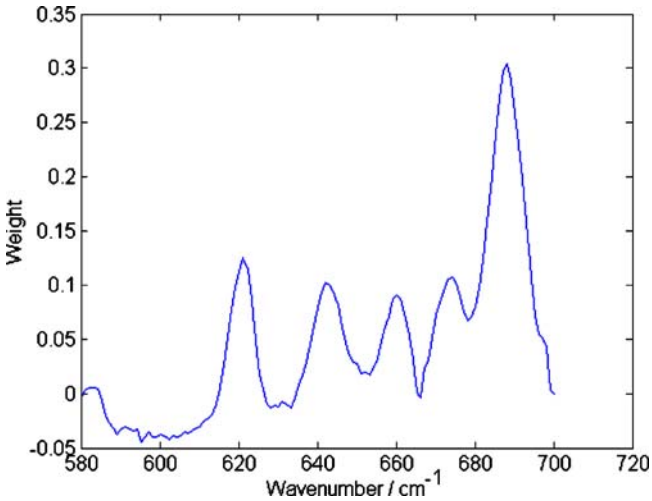

Fig. 8. Second PC loading after PCA of the Raman spectra from an Alprazolam tablet.

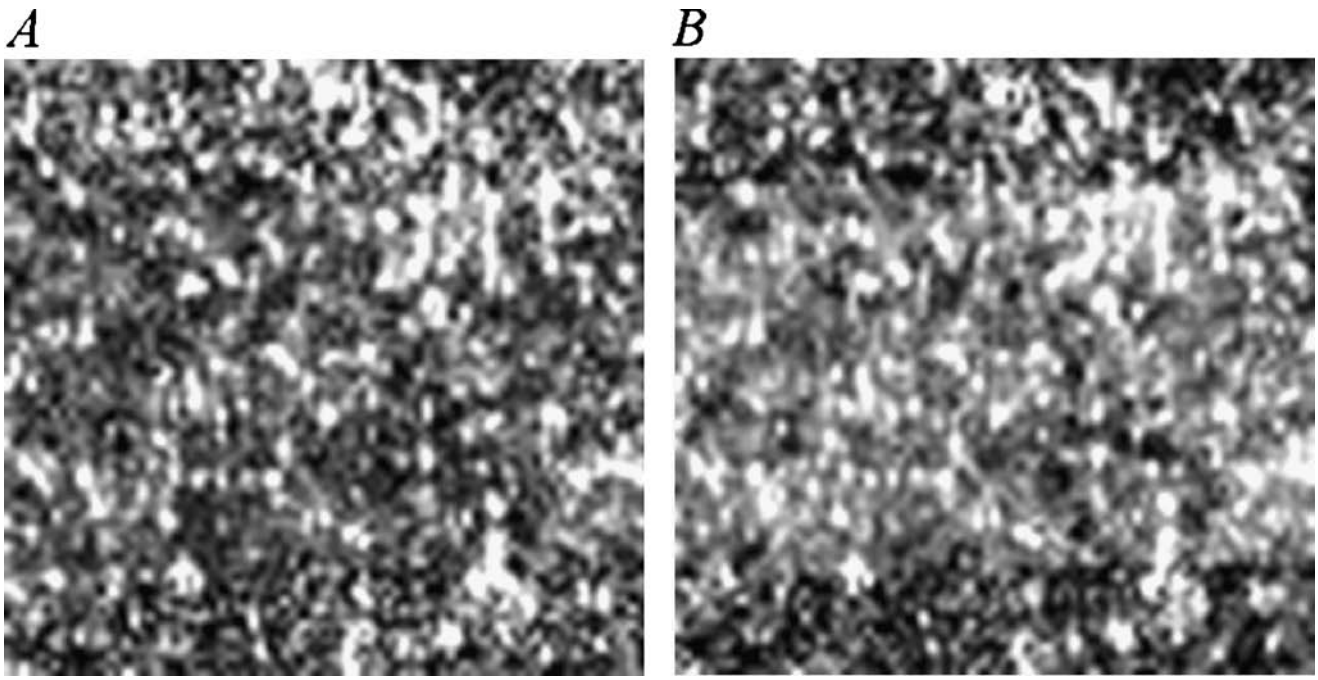

Fig. 9. Univariate (A) and second PC score images (B) of Alprazolam in an Alprazolam tablet (2×2 mm^2).

across the entire tablet in domains that do not exceed 75×75 μm^2 (which corresponds to 3×3 area in pixels).

Similar results were obtained for the other two Xanax tablets from the same batch (the good recovery one) in terms of domain size (see Fig. 7). The tablet that is described above in detail is selected because of the exemplary Raman signal obtained from it. The Raman signal from the other two tablets was not as strong which is partially evident from the data shown in Fig. 7. The same data analysis method was employed (in both cases the outlying points were found and removed) but there is an obvious difference between the highest and lowest intensity data points in one-dimensional representation of the data. Thus, the threshold for these two images had to be set to cover the data in the upper 50% of the intensity scale. Setting the same threshold as in Fig. 6 (to cover the upper 65%) would produce binarized images with too many 'on' pixels because of interference of noise. The results in Figs. 5, 6 and 7 show that one of the tablets has a stronger Raman signal of Alprazolam but the spatial distribution of Alprazolam in all three tablets is comparable, i.e., about 1% of the tablets is occupied with the domain sizes as reported above.

Comparisons between the two Alprazolam Raman images obtained in the same way from the two tablets from another batch (the bad recovery one) with the images described above reveals no significant differences. With the binarization threshold kept at about 50%, Alprazolam is again found to occupy about 1% of the total number of pixels with the domain sizes not exceeding 75 μm. The Raman

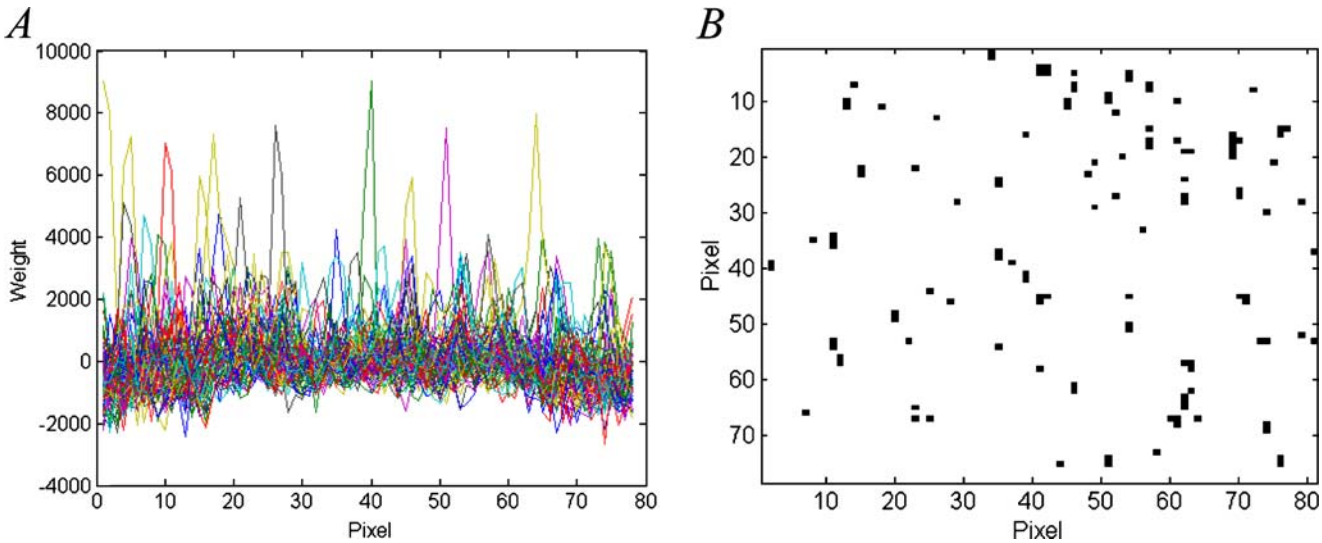

Fig. 10. One-dimensional representation of the image in Fig. 9B (A) through which the threshold for binarization is defined. The binarized image is shown in (B).

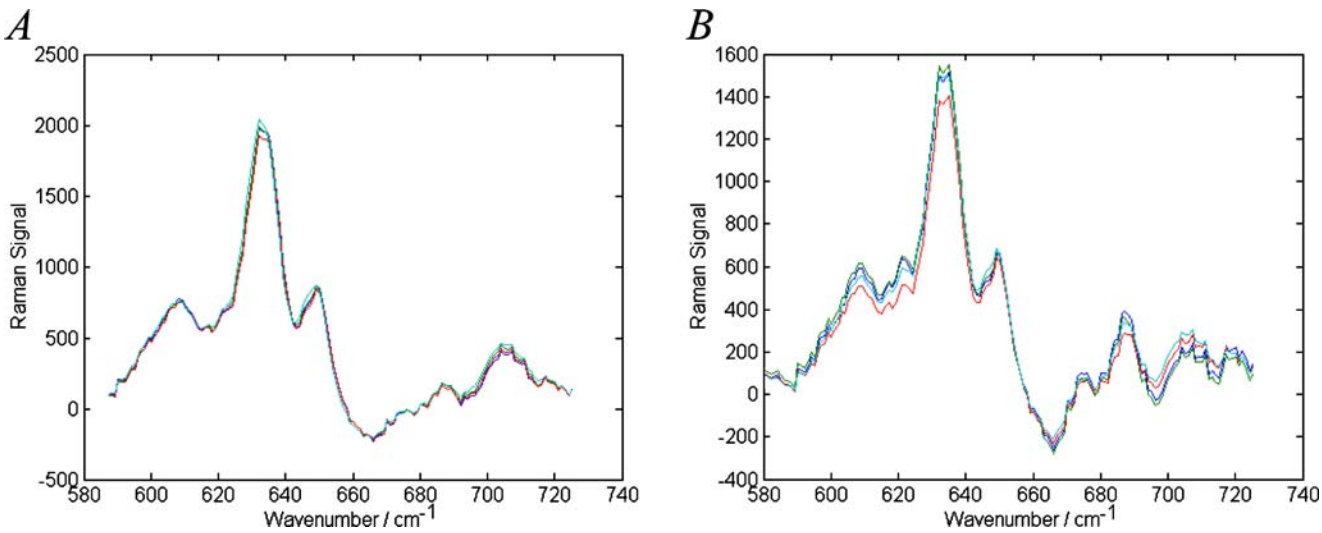

Fig. 11. Average of all the acquired mapping spectra from the Xanax (A) and Alprazolam (B) tablets.

signal from the third tablet from this batch was significantly weaker (for no clear reason) and therefore the thresholds used in the previous four cases yielded fewer pixels (0.6%) assigned to Alprazolam.

Alprazolam Tablets

The content of Alprazolam in the Alprazolam tablets is twice that of the Xanax tablets and therefore these tablets were easier to analyze. Three tablets from two batches were imaged (i.e., six in total). The data analysis approach used was the same as above. The higher intensity of the Raman signal of Alprazolam is reflected in the second PC loading (Fig. 8) that is now very similar to the Alprazolam spectrum. The strength of the Raman signal makes the univariate images at 678 cm^{-1} similar to the re-folded second PC score image in some cases (Fig. 9). Figure 10 shows the one-dimensional representation of the score image in Fig. 9. For the tablets from the first batch analyzed the Raman signal is particularly good making the difference between the extreme data points pronounced so that the binarization is facilitated (the outlying data points were again found and eliminated). For the second batch (the bad recovery one) the Raman signal was somewhat weaker so that the difference between the extreme points was not so evident but the binarization was still straightforward. The binarized images were produced with slightly varying thresholds. The decision on where to put threshold is based on one-dimensional representations as shown in Figs. 5 and 10.

The number of pixels assigned to Alprazolam in all six Alprazolam tablets was comparable, with the mean occupancy of about 1.2% (Fig. 10) of the total area. The domain sizes are still less than 3×3 pixels (75×75 μm^2). In summary, the difference between the Raman images of Alprazolam in Alprazolam and Xanax tablets is in the strength of the Raman signal and in the more abundant presence of Alprazolam in the Alprazolam tablets, while the domain sizes are found to be similar.

In the end, it is worth comparing the microscope Raman measurements with the bulk Raman measurement of the investigated tablets. The bulk Raman spectra were not collected but such a measurement is mimicked here by plotting the average spectra of the entire maps, one for each map. These spectra, each an average of more than 5,000 Raman mapping spectra, are shown in Fig. 11. The lactose features obviously dominate the spectra in Fig. 11 but the spectral indications of Alprazolam at 687 cm^{-1} are present in the Alprazolam tablets, and are much weaker in the Xanax tablets. In contrast, some of the single mapping spectra clearly feature the strong Raman response of Alprazolam. Also, the comparability of the spectra shown point out that the acquisitions were carried out under very stable conditions so that quantitative analysis are generally possible although no internal standard was used.

SUMMARY

This study demonstrates the usefulness of Raman mapping for determining spatial distributions of low-content API in commercial tablets. Alprazolam in Xanax and Alprazolam tablets (0.4 and 0.8 w/w%, respectively) was imaged via principal component scores. The Raman chemical images for the Xanax tablets could not be reliably produced via univariate methods at the position of the strongest and isolated peak of Alprazolam but PCA effectively enables the imaging due to the surprising similarity between some PC loadings and spectrum of Alprazolam. The grey-scale PC score images do not provide clear information in terms of domain size and binarization is hence employed to simplify the complexity of the PC score images. However, the binarization also fails to produce reasonable results if the binarization threshold is not carefully managed. After the binarization threshold is properly set (by eliminating the outlying points), it is found that the abundance of Alprazolam in all six tablets of Xanax and Alprazolam was very similar. The domain sizes were also found to be below 75 μm in diameter for all the tablets analyzed. The strength of the Raman signal, however, varies across the tablets so that these results depend to some extent on the threshold setting.

ACKNOWLEDGMENTS

Ian Clegg of Pfizer Inc. is thanked for thoughtful discussions. Pfizer Inc. is acknowledged for permission to publish this study.

REFERENCES

1. S. E. J. Bell, J. R. Beattie, J. J. McGarvey, K. Peters Laota, N. M. S. Sirimuthu, and S. J. Speers. Development of sampling methods for Raman analysis of solid dosage forms of therapeutic and illicit drugs. *J. Raman Spectrosc.* **35**:409 (2004).
2. S. E. J. Bell, L. J. Baret, D. T. Burns, A. C. Dennis, and S. J. Speers. Tracking the distribution of ecstasy tablets by Raman composition profiling: a large scale feasibility study. *Analyst* **128**:1331 (2003).
3. D. S. Hausman, R. T. Cambron, and A. Sakr. Application of Raman spectroscopy for on-line monitoring of low dose blend uniformity. *Int. J. Pharm.* **298**:80 (2005).
4. D. E. Bugay. Characterization of the solid-state: spectroscopic techniques. *Adv. Drug Deliv. Rev.* **48**:43 (2001).
5. G. Finni. Applications of Raman spectroscopy to pharmacy. *J. Raman Spectrosc.* **35**:335 (2004).
6. S. J. Strachan, D. Prativi, K. C. Gordon, and T. Rades. Quantitative analysis of polymorphic mixtures of carbamazepine by Raman spectroscopy and principal components analysis. *J. Raman Spectrosc.* **35**:347 (2004).
7. M. Dyrby, S. B. Engelsen, L. Nørgaard, M. Bruhn, and L. Lundsberg-Nielsen. Chemometric quantitation of the active substance (containing C≡N) in a pharmaceutical tablet using Near-Infrared (NIR) and NIR FT-Raman spectra. *Appl. Spectrosc.* **56**:579 (2002).
8. T. M. Niemczyk, M. M. Lopez-Delgado, and F. S. Allen. Quantitative determination of bucindolol concentration in intact gel capsules using Raman spectroscopy. *Anal. Chem.* **70**:2762 (1998).
9. R. L. McCreery. *Raman Spectroscopy for Chemical Analysis*, Wiley, New York, 2000.
10. P. J. Treado and M. Nelson. In J. M. Chalmers and P. R. Griffiths (eds.), *Handbook of Vibrational Spectroscopy, Vol. 2*, Wiley, New York, 2001.
11. D. A. Clark and S. Šašić. Chemical images: an introduction to technical approaches and issues. *Cytometry A* (in press). DOI: 10.1002/cyto.a.20275.
12. P. Geladi and H. Grahn. *Multivariate Image Analysis*. Wiley, New York, 1996.
13. E. R. Malinowski. *Factor Analysis in Chemistry*, 2nd ed. Wiley, New York 1991.
14. S. ŠašIć, D. A. Clark, J. C. Mitchell, and M. J. Snowden. Univariate *versus* multivariate Raman imaging—a simulation with an example from pharmaceutical practice. *Analyst* **129**:1001 (2004).
15. S. Šašić, D. A. Clark, J. C. Mitchell, and M. J. Snowden. Raman line mapping as a fast method for analyzing pharmaceutical bead formulations. *Analyst* **130**:1530 (2005).
16. P. D. A. Pudney, T. M. Hancewicz, D. G. Cunningham, and M. C. Brown. Quantifying the microstructures of soft solid materials by confocal Raman spectroscopy. *Vibr. Spectrosc.* **34**:123 (2004).
17. J. -H. Wang, P. K. Hopke, T. M. Hancewicz, and S. L. Zhang. Application of modified alternating least squares regression to spectroscopic image analysis. *Anal. Chim. Acta* **476**:93 (2003).
18. N. B. Gallagher, J. M. Shaver, E. B. Martin, J. Morris, B. M. Wise, and W. Windig. Curve resolution for multivariate images with applications to TOF-SIMS and Raman. *Chemom. Intell. Lab. Syst.* **73**:105 (2004).
19. L. Zhang, M. J. Henson, and S. S. Sekulic. Multivariate data analysis for Raman imaging of a model pharmaceutical tablet. *Anal. Chim. Acta* **545**:262 (2005).